

Supporting Information for

Optical control of protein-protein interactions via blue light induced domain swapping

Jakeb M. Reis, Darcy C. Burns & G. Andrew Woolley

Supplementary Figures:

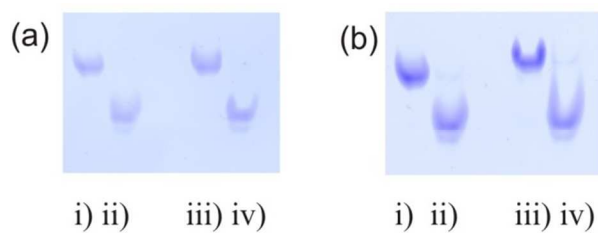


Figure S1. (a) Native PAGE analysis of c-E-helix-PYP incubated in the dark (1X TAE, 100 mM NaCl, pH 7.5, 30°C) i) 20 μ M dimer at day 0, ii) 20 μ M monomer at day 0, iii) 20 μ M after 7 days, iv) 20 μ M monomer after 7 days. Under these conditions, no appreciable interconversion is observed. (b) Incubation of c-E-helix-PYP with 1 equivalent of K-helix peptide for 30 minutes does not cause monomer-dimer interconversion. i) 20 μ M c-E-helix-PYP dimer, ii) 20 μ M c-E-helix-PYP monomer, iii) 20 μ M c-E-helix-PYP dimer + 1eq. K-helix peptide, iv) 20 μ M c-E-helix-PYP monomer + 1eq. K-helix peptide.

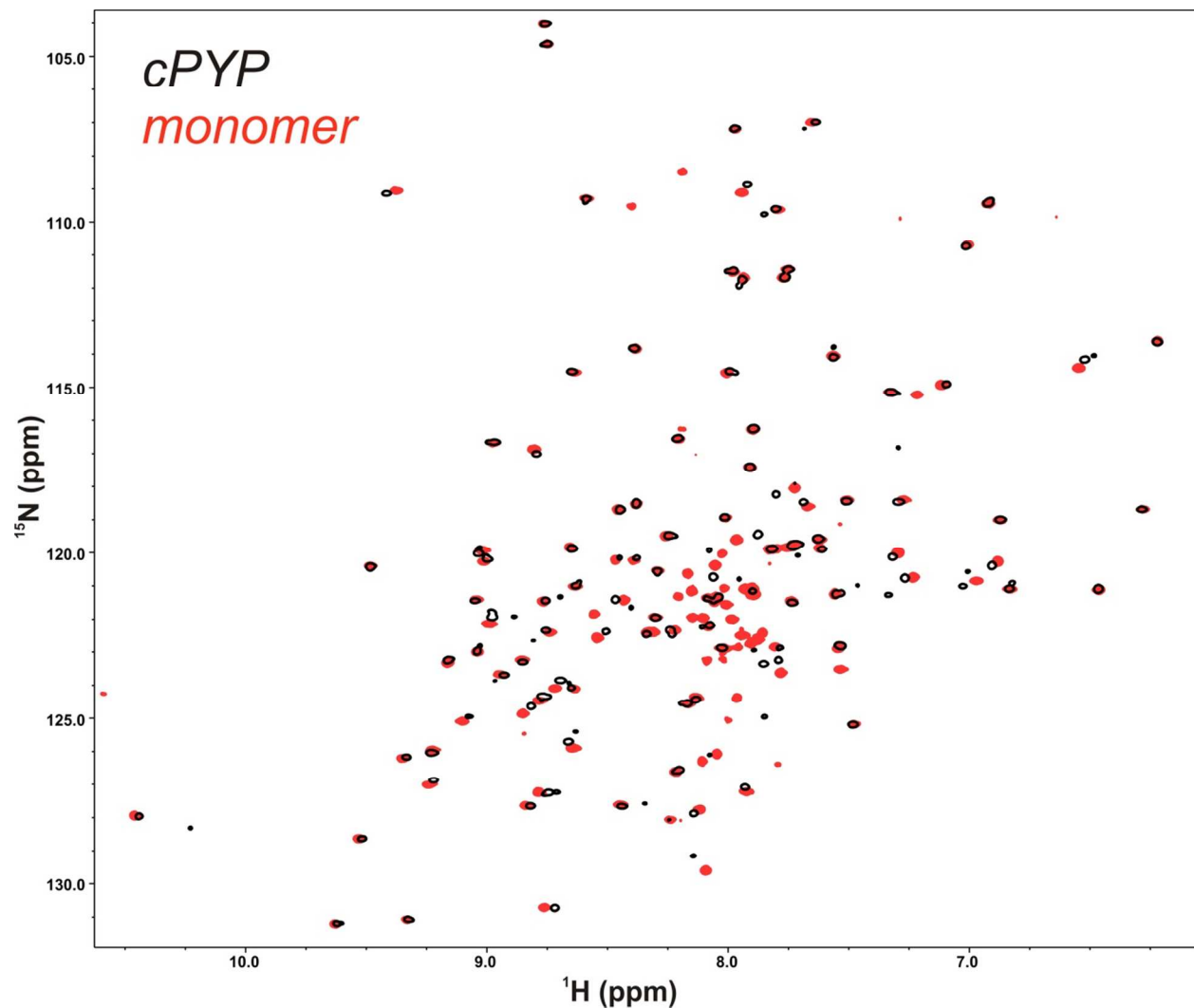


Figure S2. (a) Overlaid ^{15}NH HSQC spectra of monomeric c-E-helix-PYP (red) and c-PYP with a flexible GGSGGSGG loop insert (black). A list of overlapping resonances is provided in Table S1.

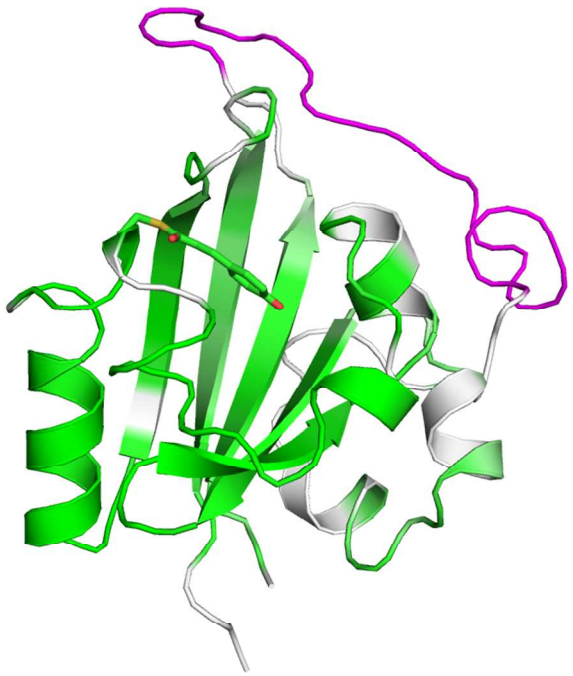


Figure S2. (b) A model of monomeric c-E-helix-PYP with residues exhibiting chemical shift overlap with cPYP colored green. Residues that are unassigned in c-E-helix-PYP are colored white. The E-helix insert (unassigned) is colored magenta.

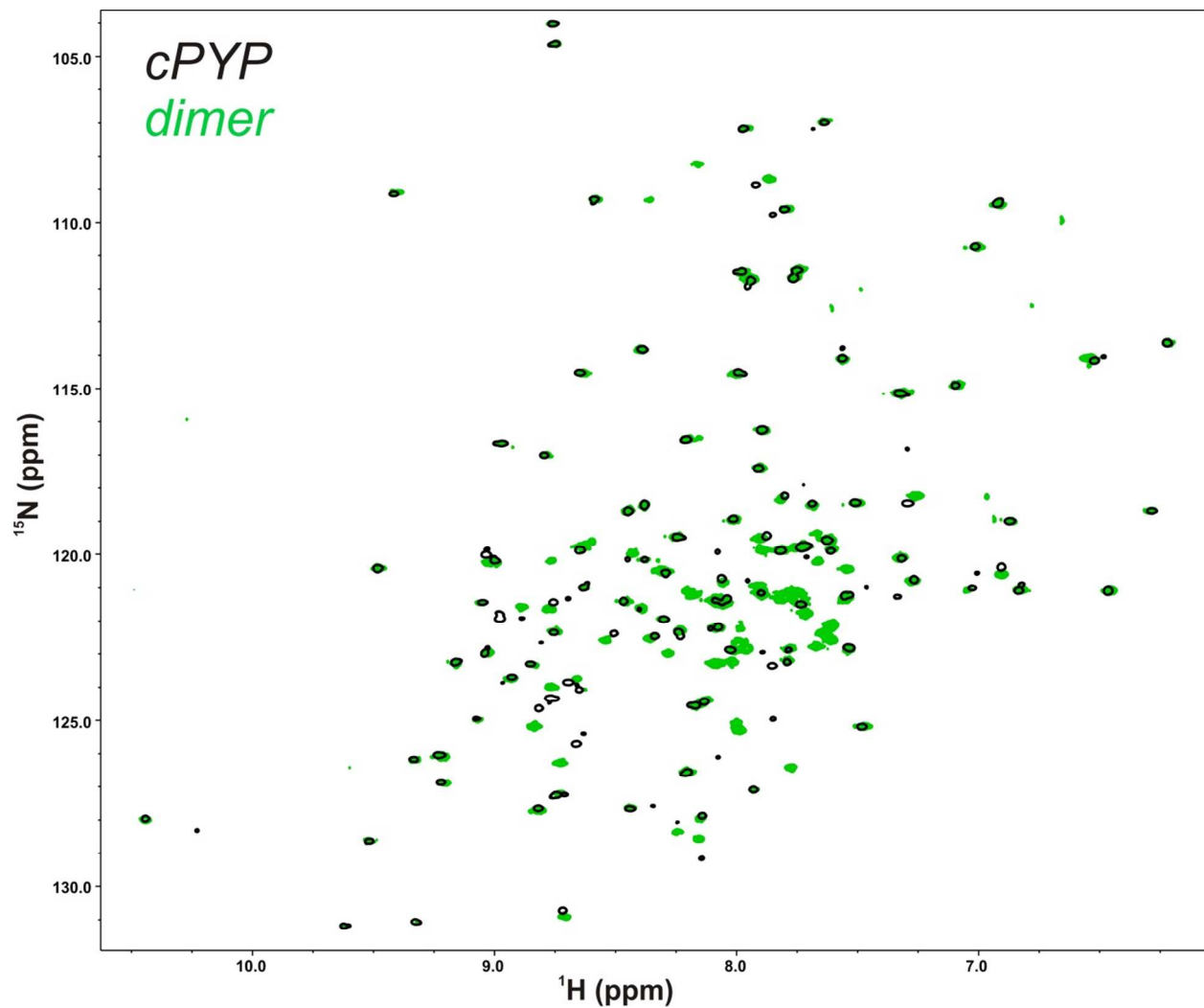


Figure S3.(a) Overlaid ^{15}NH HSQC TROSY spectra of dimeric c-E-helix-PYP (green) and c-PYP with a flexible GGSGGSGG loop insert (black). A list of overlapping resonances is provided in Table S1.



Figure S3. (b) A model of dimeric c-E-helix-PYP with residues exhibiting chemical shift overlap with cPYP colored green. Residues that are unassigned in c-E-helix-PYP are colored white. The E-helix insert (unassigned) is colored magenta.

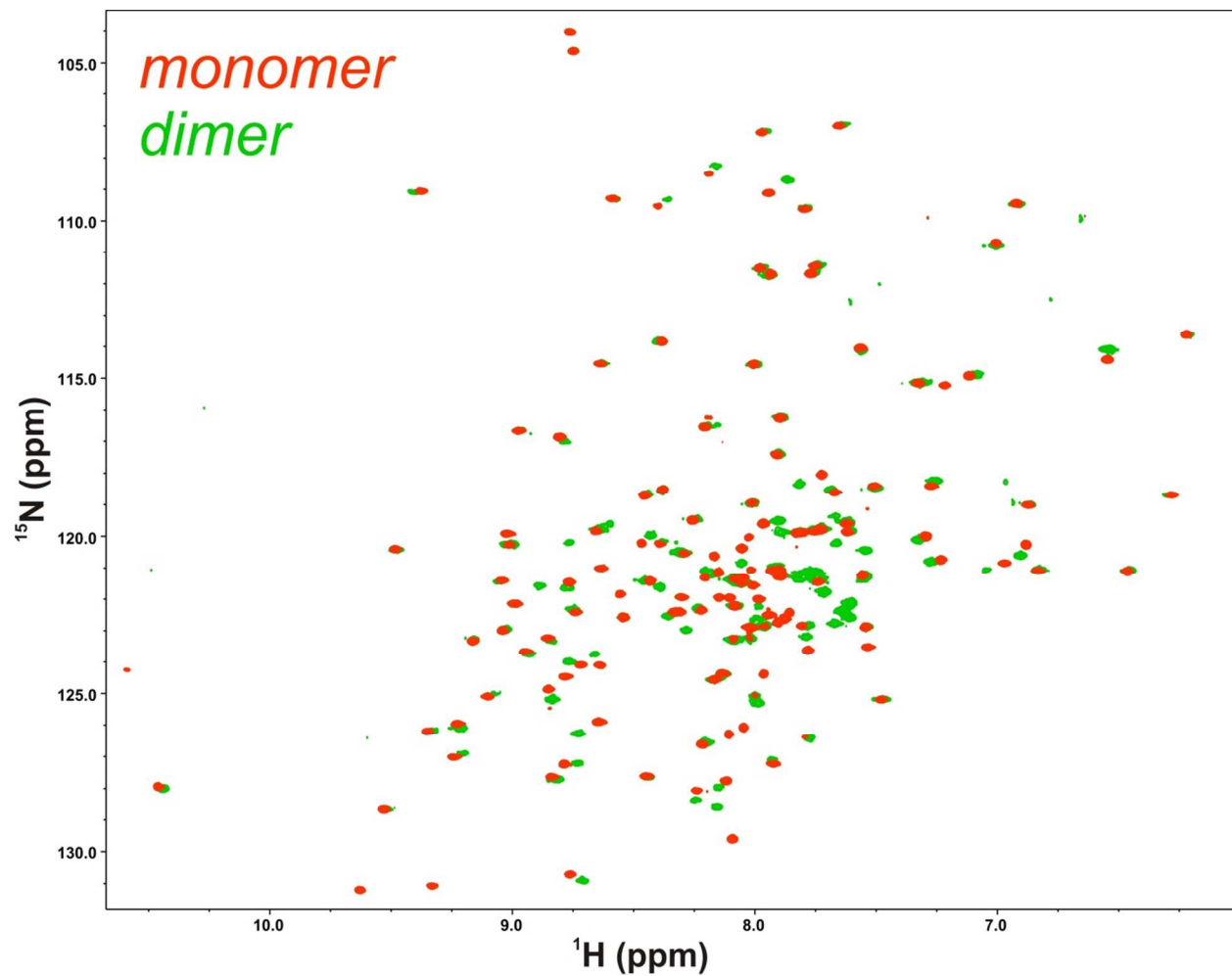


Figure S4. ^{15}NH HSQC TROSY of c-E-helix-PYP monomer (red) and dimer (green) showing overlap of resonances.

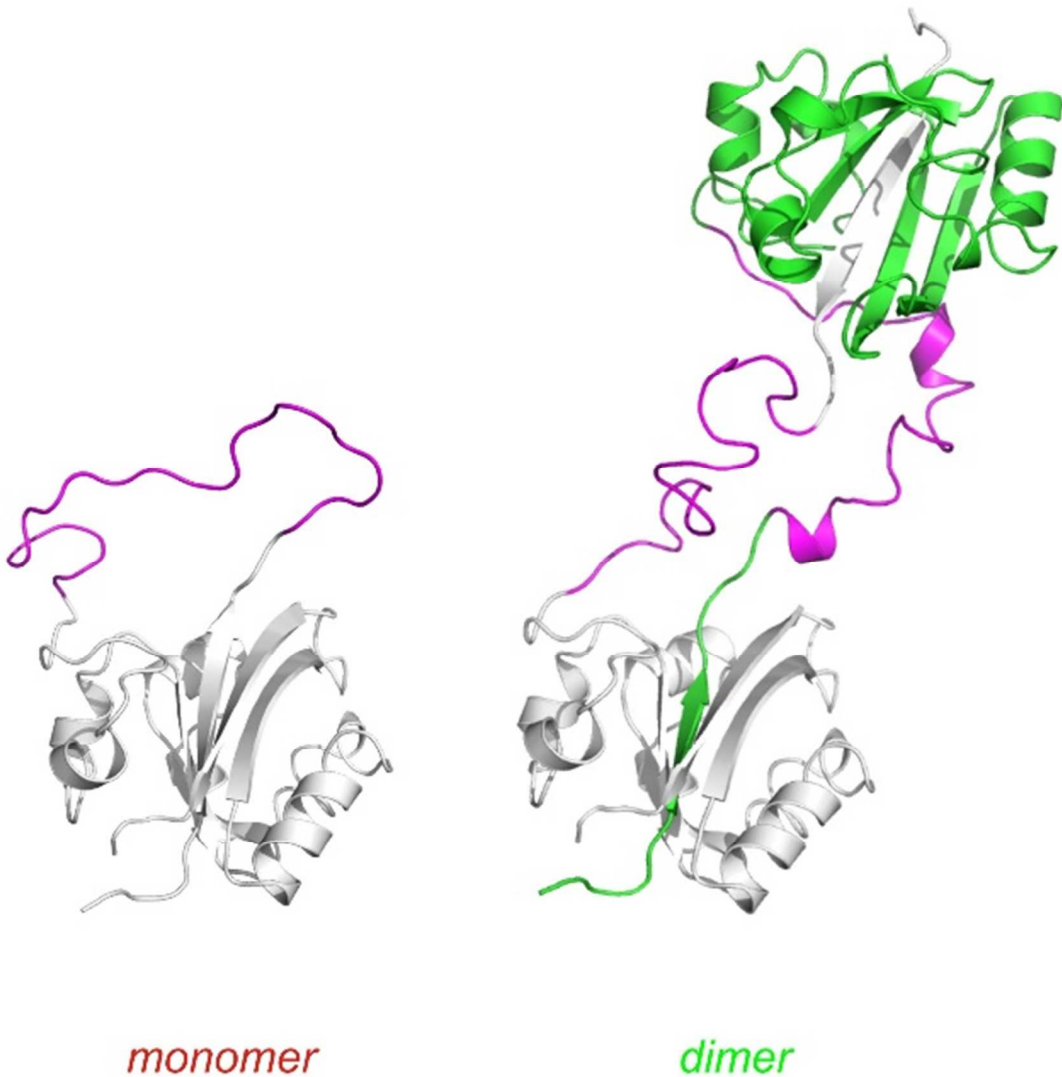


Figure S5. Models of the c-E-helix-PYP monomer and the proposed domain swapped dimer. The E-helix loop insertion is colored magenta in each case. Signals from these residues map to differences in the HSQC spectra of monomer and dimer (near the center or the spectrum). In the dimer, this sequence hinges to allow for swapping of N-terminal beta strands. In the dimer, one monomer is colored green for clarity. Models are based on the X-ray crystal structure of wild-type PYP (PDB code: 1 NWZ). Linkers were modeled using the loop modeler algorithm in Accelrys Discovery Studio protein modeling software. In the dimer structure, weak constraints on the torsion angles of the linker region were imposed to promote the formation of helical structure (as suggested by the CD data). The distance between monomers and the relative orientations of monomers in the dimer are arbitrary.

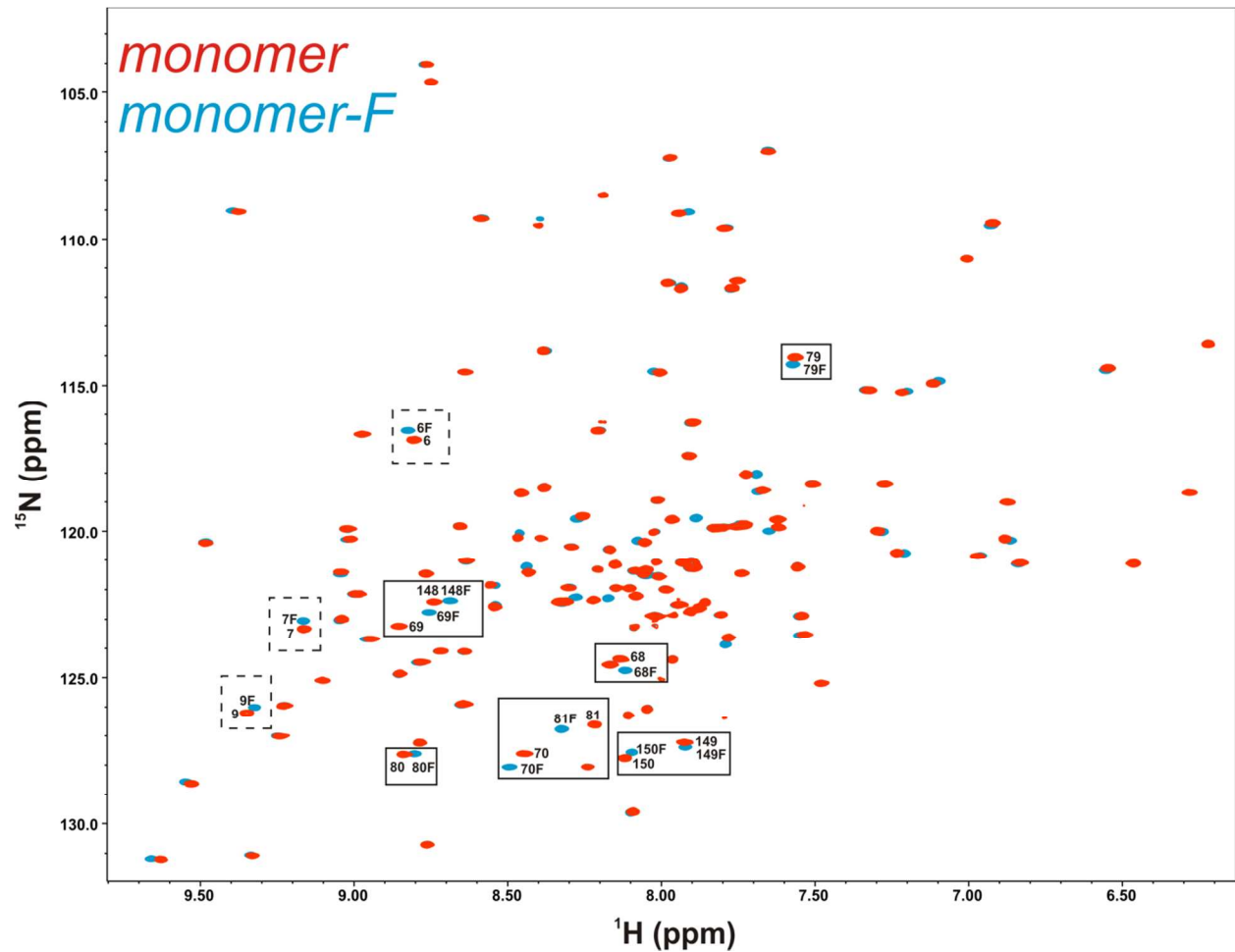


Figure S6 ^{15}NH HSQC TROSY of the c-E-helix-PYP monomer (red) and the monomer containing 5-FTrp (blue). A small subset of resonances are affected by fluorine substitution. Crosspeaks boxed with dashed lines indicate residues on the same β strand as the 5-fluorotryptophan substitution; those boxed with solid lines indicate residues on the adjacent β strands.

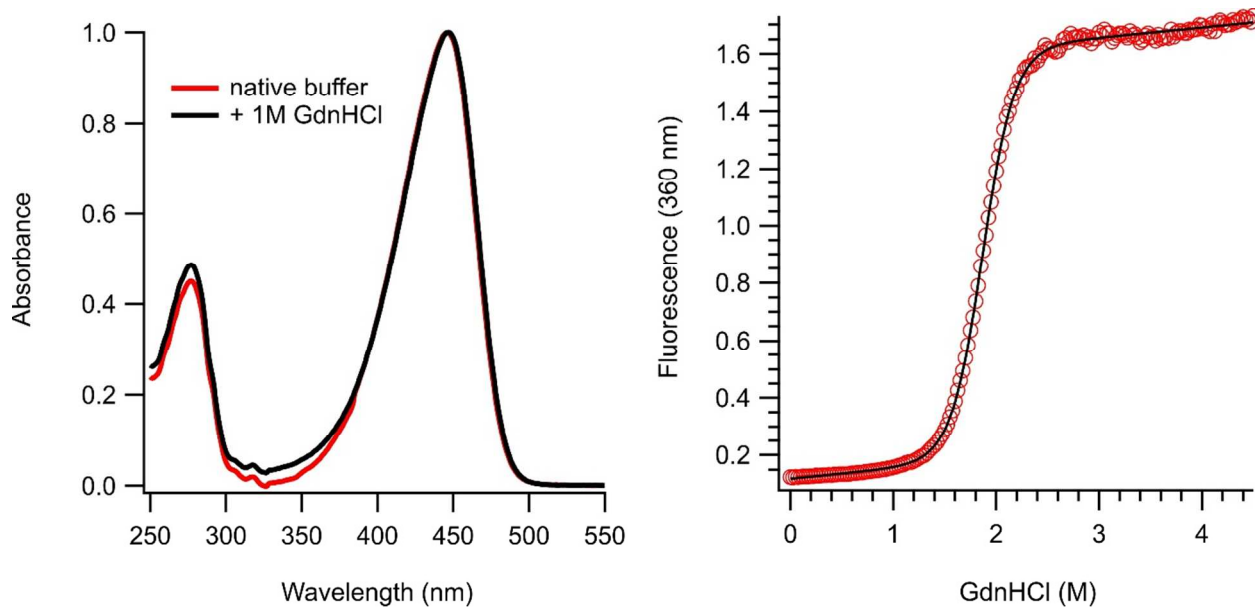


Figure S7. The addition of 1M GdnHCl does not cause complete denaturation of the protein as evidenced by the persistence of a normal UV-Vis absorbance trace 1X TAE 100 mM NaCl pH 7.5, 30°C (a). A GdnHCl induced denaturation transition is seen at ~2M when monitored using intrinsic fluorescence (α -E-helix-PYP monomer, dark adapted, 5 μ M, 1X TAE 100 mM NaCl pH 7.5, and 25°C).

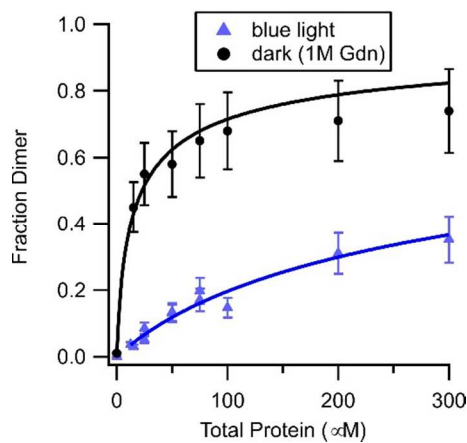


Figure S8. Fraction of dimer observed at equilibrium vs. total protein concentration under blue light or under dark conditions in the presence of 1 M Gdn HCl (1X TAE, 100 mM NaCl, pH 7.5 30°C). Data are fitted to the equation:

$$\text{fraction dimer} = \frac{2 * ((4 * [\text{total protein}]) + (2 * K_d) - (((4 * [\text{total protein}]) + (2 * K_d))^2 - (16 * [\text{total protein}]^2)^{0.5}))}{(8 * [\text{total protein}])}$$

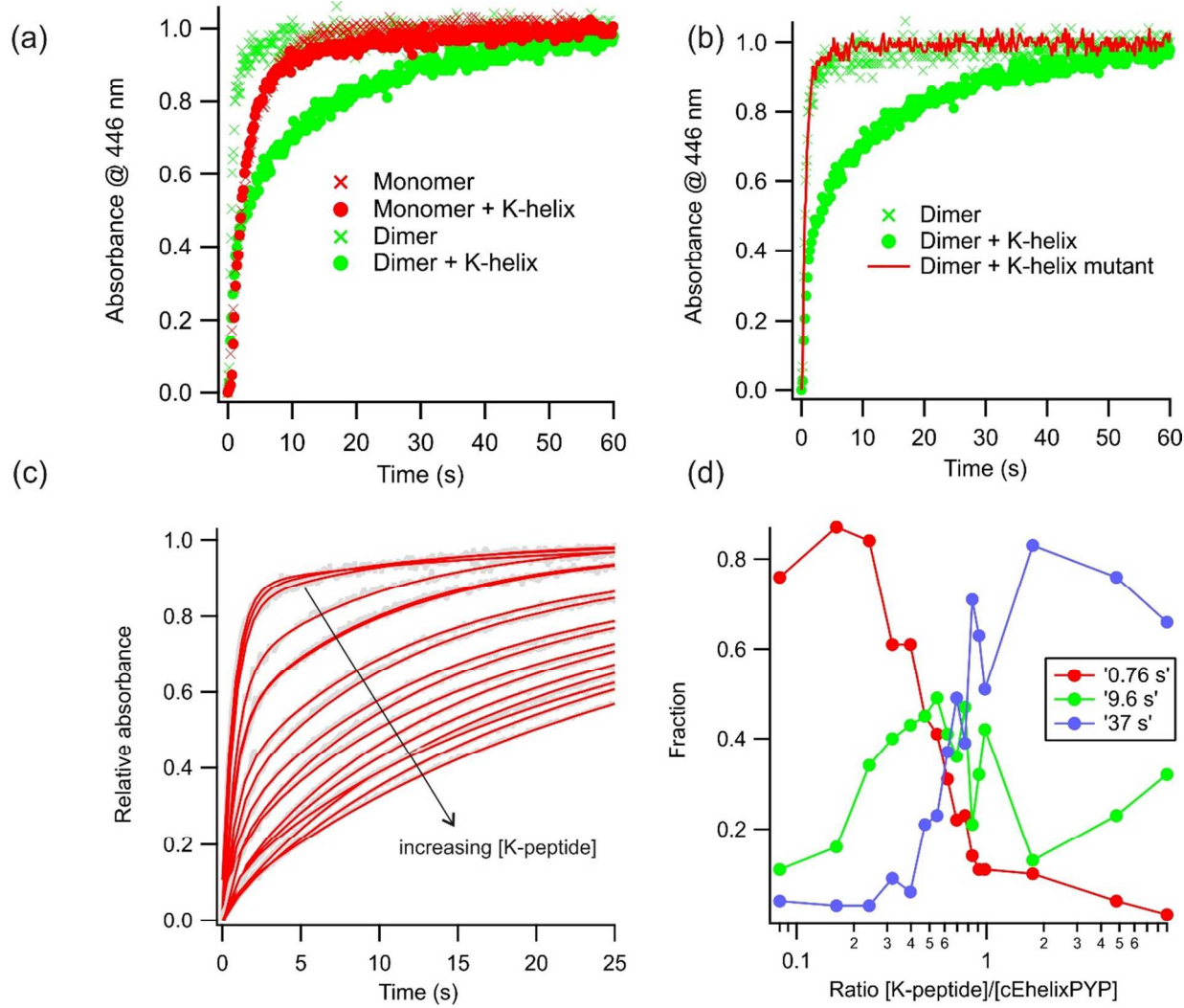


Figure S9. (a) Thermal recovery of c-E-helix-PYP monomer and dimer in the absence and presence of K-helix peptide. Only the dimer relaxation rate is affected (~15-fold slower)(b) Thermal recovery of c-E-helix-PYP dimer in the absence and presence of K-helix peptide bearing two Leu-to-Ala mutations. No effect on relaxation is seen. (c) Thermal recovery of the c-E-helix-PYP dimer with increasing concentrations of K-peptide. The data are globally fit using a triple exponential function describing a slow, intermediate, and fast relaxation process. (d) Fractions of each relaxation component are plotted as a function of the K-peptide/ c-E-helix-PYP ratio. These data are consistent with a free dimer, a dimer with one K-peptide bound and a dimer with two K-peptides bound each exhibiting a unique relaxation rate.

Table S1. List of overlapping ^1H - ^{15}NH resonances between cPYP, c-E-helix-PYP monomer and c-E-helix-PYP dimer. cPYP resonances were previously assigned using standard triple resonance experiments (1). Chemical shift differences of c-E-helix-PYP monomer and dimer, with respect to cPYP are shown.

c-E-helix-PYP									
Residue Number		cPYP		Monomer		Dimer		$(5 \times \Delta\delta ^1\text{H}) + (\Delta\delta ^{15}\text{N})$	
cPYP	c-E-helix-PYP	$\delta^1\text{H}$	$\delta^{15}\text{N}$	$\delta^1\text{H}$	$\delta^{15}\text{N}$	$\delta^1\text{H}$	$\delta^{15}\text{N}$	Monomer	Dimer
5	5	7.99	114.51	8.01	114.56	8.00	114.56	0.11	0.07
6	6	8.80	117.01	8.81	116.88	8.79	117.00	0.18	0.04
7	7	9.16	123.25	9.16	123.33	9.16	123.27	0.10	0.03
8	8	9.05	121.44	9.05	121.41	9.05	121.44	0.06	0.01
9	9	9.33	126.17	9.35	126.20	9.33	126.19	0.10	0.03
10	10	8.93	123.69	8.95	123.67	8.93	123.76	0.11	0.08
11	11	8.66	125.71	8.65	125.90	8.73	126.27	0.28	0.87
12	12	8.82	124.64	8.85	124.86	8.84	125.19	0.38	0.65
13	13	7.85	123.36	ND	ND	ND	ND	ND	ND
23	40	7.79	123.23	ND	ND	ND	ND	ND	ND
24	41	7.77	126.44	7.80	126.39	7.77	126.42	0.16	0.03
25	42	7.34	121.27	ND	ND	ND	ND	ND	ND
26	43	8.14	129.16	8.09	129.61	8.15	128.57	0.70	0.64
35	52	7.69	118.47	7.67	118.61	7.68	118.53	0.22	0.08
37	54	7.27	120.77	7.23	120.75	7.27	120.80	0.19	0.07
38	55	7.10	114.91	7.12	114.93	7.09	114.89	0.11	0.07
39	56	7.32	120.13	7.30	119.99	7.32	120.11	0.24	0.03
40	57	8.24	122.34	8.22	122.35	8.24	122.29	0.10	0.07
41	58	8.45	120.16	8.47	120.23	8.43	119.96	0.16	0.29
42	59	8.38	109.35	8.40	109.54	8.36	109.32	0.29	0.15
44	61	8.23	122.46	ND	ND	ND	ND	ND	ND
45	62	7.80	118.24	7.72	118.06	7.82	118.34	0.56	0.18
46	63	7.92	108.87	7.94	109.12	7.87	108.69	0.36	0.46
47	64	6.91	120.39	6.88	120.27	ND	ND	0.25	ND
48	65	8.51	122.39	8.54	122.59	8.54	122.59	0.37	0.38
49	66	6.52	114.16	6.55	114.41	6.54	114.10	0.36	0.15
50	67	9.42	109.14	9.38	109.06	9.41	109.09	0.28	0.07
51	68	8.14	124.43	8.13	124.36	8.12	124.39	0.08	0.10
52	69	8.85	123.30	8.86	123.23	8.84	123.33	0.09	0.10
53	70	8.44	127.66	8.45	127.61	8.44	127.64	0.09	0.03
54	71	9.52	128.62	9.53	128.64	9.52	128.61	0.07	0.01
55	72	8.25	119.47	8.26	119.48	8.25	119.46	0.07	0.01
56	73	8.76	104.03	8.76	104.04	8.76	104.02	0.03	0.02

57	74	7.91	117.41	7.91	117.42	7.90	117.40	0.02	0.05
58	75	8.59	109.30	8.59	109.29	8.58	109.30	0.01	0.05
59	76	9.04	122.98	9.04	122.99	9.03	122.96	0.02	0.07
60	77	8.63	120.99	8.63	121.01	8.63	121.01	0.03	0.03
61	78	9.62	131.19	9.63	131.20	9.62	131.18	0.04	0.01
62	79	7.56	114.10	7.57	114.05	7.56	114.12	0.06	0.04
63	80	8.82	127.65	8.84	127.63	8.82	127.71	0.12	0.06
64	81	8.20	126.56	8.22	126.61	8.21	126.56	0.13	0.02
65	82	8.47	121.41	8.43	121.42	8.46	121.41	0.19	0.06
66	83	7.88	119.45	7.97	119.60	7.90	119.51	0.59	0.19
67	84	7.61	119.89	7.62	119.87	7.60	119.84	0.07	0.09
68	85	7.64	106.99	7.65	106.99	7.64	106.95	0.09	0.06
71	88	7.97	107.18	7.97	107.20	7.96	107.18	0.02	0.05
72	89	8.65	114.52	8.64	114.54	8.63	114.54	0.06	0.09
73	90	7.53	122.82	7.54	122.88	7.54	122.88	0.12	0.08
74	91	8.30	121.96	8.30	121.94	8.30	121.95	0.03	0.02
76	93	7.94	111.75	7.94	111.70	7.94	111.73	0.07	0.05
77	94	7.90	116.25	7.90	116.28	7.89	116.26	0.04	0.04
78	95	6.92	109.43	6.92	109.45	6.92	109.46	0.02	0.05
79	96	6.84	121.08	6.83	121.09	6.83	121.05	0.03	0.08
80	97	8.97	116.65	8.97	116.68	8.97	116.66	0.05	0.01
81	98	7.73	119.78	7.73	119.79	7.72	119.76	0.02	0.06
82	99	9.48	120.42	9.48	120.40	9.48	120.41	0.02	0.04
83	100	9.33	131.05	9.33	131.07	9.32	131.04	0.04	0.08
84	101	6.22	113.64	6.22	113.61	6.21	113.62	0.04	0.05
85	102	7.77	111.68	7.77	111.69	7.76	111.64	0.03	0.07
87	104	6.87	118.99	6.87	119.00	6.87	118.99	0.02	0.03
88	105	7.82	119.88	7.83	119.89	7.82	119.90	0.04	0.03
90	107	8.38	118.51	8.38	118.53	8.38	118.52	0.03	0.03
91	108	8.21	116.54	8.21	116.56	8.20	116.52	0.03	0.07
92	109	7.48	125.19	7.48	125.19	7.47	125.19	0.02	0.06
93	110	8.29	120.55	8.29	120.54	8.31	120.50	0.01	0.12
95	112	8.39	113.83	8.38	113.84	8.40	113.85	0.02	0.06
96	113	7.51	118.44	7.51	118.40	7.50	118.46	0.04	0.05
97	114	8.65	124.08	8.64	124.09	ND	ND	0.06	ND
98	115	8.75	104.62	8.75	104.63	8.74	104.62	0.03	0.02
99	116	6.47	121.09	6.46	121.12	6.48	121.11	0.05	0.10
100	117	8.03	122.89	8.02	122.88	8.01	122.89	0.01	0.07
101	118	8.45	118.70	8.46	118.70	8.44	118.68	0.04	0.06
102	119	7.63	119.57	7.62	119.60	7.61	119.56	0.04	0.07
103	120	7.80	109.61	7.80	109.62	7.79	109.59	0.05	0.06
104	121	8.17	124.55	8.17	124.56	8.16	124.55	0.02	0.04
105	122	7.55	121.25	7.56	121.24	7.54	121.24	0.03	0.06
106	123	7.98	111.48	7.98	111.51	7.97	111.51	0.05	0.06
107	124	7.75	111.44	7.75	111.43	7.74	111.41	0.02	0.10

108	125	8.01	118.93	8.01	118.94	8.01	118.95	0.02	0.03
109	126	7.79	122.87	7.81	122.85	7.78	122.84	0.12	0.06
111	128	9.00	120.20	9.01	120.26	9.00	120.23	0.14	0.05
112	129	8.24	128.07	8.24	128.07	8.25	128.36	0.03	0.30
113	130	8.76	121.44	8.77	121.46	8.77	121.63	0.07	0.25
114	131	8.65	119.87	8.66	119.82	8.64	119.78	0.09	0.14
115	132	9.23	126.04	9.23	125.96	9.22	126.09	0.10	0.12
116	133	7.30	118.46	7.28	118.40	7.26	118.24	0.16	0.42
117	134	8.75	127.26	8.79	127.23	8.73	127.21	0.21	0.14
118	135	7.74	121.50	7.74	121.45	7.74	121.35	0.08	0.18
119	136	6.29	118.69	6.28	118.68	6.29	118.68	0.02	0.02
121	138	7.01	110.73	7.01	110.70	7.01	110.75	0.07	0.05
122	139	8.38	120.16	8.39	120.23	8.38	120.17	0.15	0.02
124	141	8.70	123.85	8.72	124.09	8.77	123.99	0.36	0.50
125	142	8.72	130.73	8.76	130.71	8.71	130.90	0.24	0.21
126	143	9.04	120.02	9.02	119.91	ND	ND	0.17	ND
127	144	8.98	121.94	8.99	122.14	ND	ND	0.27	ND
128	145	8.77	124.32	8.78	124.46	ND	ND	0.22	ND
129	146	9.22	126.87	9.24	127.01	9.20	126.90	0.25	0.13
130	147	9.08	124.95	9.10	125.09	9.08	124.98	0.27	0.06
131	148	8.76	122.35	8.74	122.41	8.75	122.31	0.13	0.09
132	149	7.93	127.08	7.93	127.22	7.93	127.10	0.16	0.01
133	150	8.14	127.87	8.12	127.75	8.15	127.96	0.23	0.10
134	151	8.34	122.47	8.32	122.41	8.35	122.53	0.15	0.13
136	153	8.63	125.40	ND	ND	ND	ND	ND	ND
139	156	7.96	122.87	7.96	122.87	7.96	122.84	0.01	0.08
141	158	7.90	121.15	ND	ND	ND	ND	ND	ND
142	159	8.09	121.38	8.09	121.36	8.09	121.37	0.03	0.01

Table S2. List of ^{15}N -NH chemical shifts that are perturbed by 5-fluorotryptophan incorporation. $\Delta\delta$ is the difference in chemical shift between non perturbed (*i. e.* ^{15}N Only) and perturbed (^{15}N , 5-FTr labelled) chemical shifts. Chemical shifts from residues on the same β strand as the fluorine substitution are not expected to be perturbed in the dimer (N.E.)

Residue	$\Delta\delta^{15}\text{N} + (5 \times \Delta\delta^1\text{H})$ (ppm)	
Monomer		Dimer
5-SER	0.430	N.E.
7-TRP	0.292	N.E.
9-PHE	0.285	N.E.
68-ALA	0.482	0.426
69-ILE	0.968	0.943
70-GLN	0.695	0.751
79-GLN	0.268	0.326
80-TYR	0.193	0.181
81-ASN	0.700	0.775
148-LYS	0.306	0.252
149-LYS	0.182	N.D.
150-ALA	0.307	0.359

References

1. Kumar AB, D. C.; Al-Abdul-Wahid, M. S.; Woolley G. A. (2013) A Circularly Permuted Photoactive Yellow Protein as a Scaffold for Photoswitch Design. *Biochemistry* 52(19):3320-3331.